PHYSICAL REVIEW B VOLUME 26, NUMBER 4 15 AUGUST 1982

# Motion of interstitials in metals: Quantum tunneling at low temperatures

H. R. Schober
*Institut für Festkörperforschung der Kernforschungsanlage, Postfach 1913, 5170 Jülich, West Germany*

A. M. Stoneham
*Theoretical Physics Division, AERE Harwell, Oxon OX11 ORA., England*
(Received 23 September 1981)

Tunneling rates for heavy-impurity interstitials in fcc metals are calculated. The full interstitial—host-lattice coupling is taken into account in the dynamics as well as in the lattice relaxation. It is shown that resonant modes play a decisive role in tunneling. The results of this full dynamical study are compared to simple one-dimensional models, from which it appears that the one-dimensional approximation can be used to extrapolate to different values of mass, jump distance, and classical activation energy. The method can be extended to study the finite-temperature behavior, and we indicate how this can be done.

## I. INTRODUCTION

It is well known that self-interstitials and heavy-impurity interstitials (e.g., Fe in Al) in metals are mobile at very low temperatures. In some cases (e.g., Au self-interstitial) the interstitials appear to be mobile at the lowest temperatues studied, typically around 1 K; in other cases (e.g., self-interstitials in Cu and Al) there is a threshold, typically 20—40 K, above which the mobility rapidly increases. The rapid annihilation prevents a detailed study of the temperature dependence of the mobility of self-interstitials. The most important experimental studies are, therefore, done on trapped-impurity interstitials. The main techniques are internal friction and Mössbauer effect.

Most interpretations of the data are classical, i.e., in terms of hopping motion described approximately by an Arrhenius expression of the form

$$W = W_0 \exp(-\epsilon/kT) \, . \tag{1.1}$$

Clearly this will not describe cases where motion occurs down to the lowest temperatures known. In those circumstances one must consider the effects of tunneling and the quantum corrections this implies. It is these quantum effects which are the subject of the present paper. We consider them in several stages. Firstly, we have made classical calculations of the equilibrium geometries and classical activation energies of self- and impurity interstitials with the use of empirical interatomic potentials. Secondly, we have calculated quantum tunneling rates at $T=0$ in the same model, with minimal extra approximations. The finite temperature rates present a formidable technical problem and we merely indicate the way they can be obtained. The outline of the way in which quantal behavior can be handled is one of the main purposed of our paper. Thirdly, we have calculated the $T=0$ tunneling rates using the simple models usually invoked. These "model" rates, normally based on one-dimensional potentials as a function of some reaction coordinate, are expressed in terms of a classical activation energy and a classical force constant near equilibrium. The comparison of the model predictions and the full quantal results are the second major purpose of this paper.

## II. INTERSTITIAL IMPURITY COMPLEXES

### A. Models for trapped interstitials

The two techniques which have been especially important in analyzing the structure of interstitial impurity pairs have been measurements of Mössbauer intensity and of internal friction. The early work on the change in Mössbauer intensity in Al:Fe (Refs. 1 and 2) between 15 and 20 K was interpreted at first[3] in terms of jumps confined to an octahedral cage of positions.[4]

Later measurements of the direction dependence in single crystals[5] ruled this out and a cubic cage was proposed instead. Meanwhile, internal friction

showed a number of low-energy relaxation peaks in many different systems.[6] The relaxation of Al:Fe seems to behave classically at the experimental frequencies and temperatures.[7] The internal friction results on Al:Zn, on the other hand, suggest an octahedral cage with relaxation via a tunneling process.[8] Tunneling phenomena are also observed in amorphous metals and in low-temperature creep of metals.[9] An interesting feature of the internal friction is the occurrence of pairs of relaxation peaks showing an exactly parallel annealing behavior (frozen-to-free split-interstitial phenomenon). Several models have been proposed to explain the experimental results. None of these models explains the apparent frozen-to-free behavior of the split interstitial, and one has to assume that two different defects accidentally anneal in parallel ways.[7] We have therefore done the calculations for three different models.

### B. Interatomic potentials

We have used short-range potentials for the interactions between host atoms and between the impurity and its neighbors. Since impurities in Al have been studied most intensively we have modeled impurity Al systems.

In order to get realistic quantitative values it is necessary to reproduce the known activation energies and relaxation values. Most published Al potentials give values too low for the activation energy of the self-interstitial, and relaxation volumes are often not even calculated. We have taken for the host-host interaction, $V(R)$, with $R < 1.2a$, the modified Morse potential:

$$V(R)=V_0+D\{\exp[-2\alpha(R-R_0)] -2\exp[-\alpha(R-R_0)]\} -C(R-R_{\mathrm{NN}})^4\Theta(R_{\mathrm{NN}}-R),\quad R<1.2a \tag{2.1}$$

where NN stands for nearest neighbor, $V_0=0.0233$ eV, $R_0=0{:}71555a=2.89$ Å for Al, $D=0.227$ eV, $R_{\mathrm{NN}}=a/\sqrt{2}=2.86$ Å for Al, $a=4.04$ Å for Al, $C=1200$ eV, $\alpha=7.6499a^{-1}=1.89$ Å$^{-1}$ for Al, and $\Theta(x)$ is the Heaviside function. This potential was originally derived for Cu[4], though it is known too to describe interstitials and their conglomerates in Al.[10] It also gives reasonable values for the elastic constants if scaled by the appropriate lattice constant ($a=4.04$ Å) and mass ($m=27$) for Al.

The impurity-host interactions used the same potential with the replacement of $R$ by $R+\delta$. As $\delta$ varies one mimics the change of impurity "size."[4]

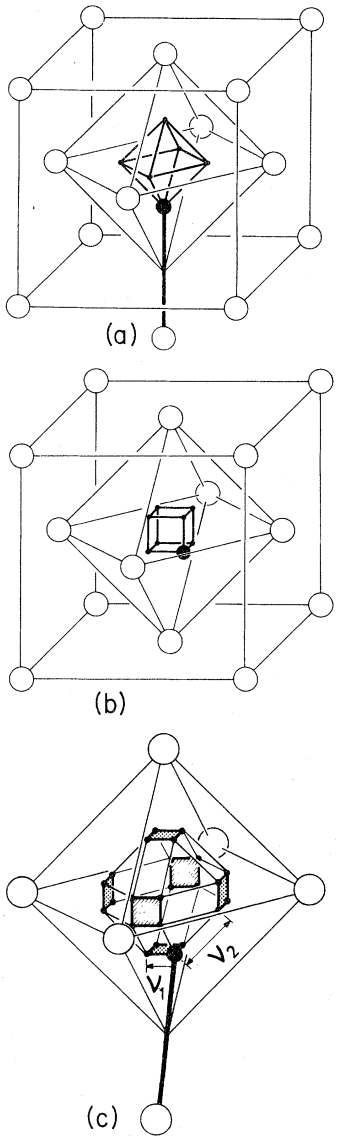


FIG. 1. Possible configurations for heavy impurity interstitials in fcc metals: (a) mixed dumbbell (octahedral cage), (b) cubic cage, and (c) tilted mixed dumbbell (split-octahedral cage).

### C. Static calculation

We have calculated equilibrium configurations and energies at $T=0$ K for a range of values of $\delta$ using the DEVIL code originally developed at Harwell. For details of the calculation procedure see, e.g., Ref. 11.

For $\delta=0$, the self-interstitial, one obtains the

⟨100⟩ dumbbell as the stable configuration, in accordance with the experiment. This dumbbell can migrate by a rotation-translation jump process with a classical activation energy of $E_a = 120$ meV. For an impurity atom, this jump process does not lead to long-range migration, but merely to motion in a cage of equivalent sites surrounding the octahedral position [see Fig. 1(a)]. With increasing values of the impurity size $\delta$ the configuration stays essentially the same (mixed ⟨100⟩ dumbbell) with the impurity moving closer to the octahedral site, the cage becoming smaller, and the classical activation energy $E_a$ falling to about 1 meV as $\delta$ approaches $0.03a$. The energy surface still shows clearly defined minima separated by saddle points. This geometry seems to be realized in Al:Zn.[8] For $\delta \sim 0.03a$ the ⟨100⟩ dumbbell becomes unstable, and the impurity occupies a position displaced by $(\epsilon,\epsilon,\epsilon)$ from the octhaedral site. The equivalent impurity sites form a cubic cage [Fig. 1(b)]. This configuration has been proposed for Al:Fe.[5] The energy surface no longer shows clearly defined minima and saddle points, but has multitude of local minima, etc. For $\delta > 0.05a$ the impurity sits in the octahedral site, and there is no longer a cage motion.

It has been shown that self-interstitials and ⟨100⟩ mixed dumbbells have low-energy resonant libration modes.[12] A small perturbation of the potential can make this resonant mode unstable, so that the ⟨100⟩ mixed dumbbell tilts [Fig. 1(c)].[13] The impurity atom can jump with a jump frequency $\nu_1$ ($E_a$ is typically less than about 10 meV) between the four sites surrounding the untilted position, and with a frequency $\nu_2$ ($E_2 \approx 50$ meV typically) from one ring of four sites to the next one. Such tilts can be induced, e.g., by an additional term $V_{\text{add}}$ in the host-impurity potential (see Fig. 2):

$$V_{\text{add}} = A \exp\left[\frac{(R-R_0)^2}{b^2}\right] \tag{2.2}$$

with

$$A \approx 0.02\ldots0.05\ eV\ ,$$

$$b \approx 0.02\ldots0.05a\ ,$$

$$R_0 \approx 0.6a\ .$$

Such a tilted-dumbbell configuration (split-octahedral cage) is a possible alternative model for the Al:Fe system.

The octahedral and cubic cages have also been found for a range of impurity interstitials in Al by computer simulations using pair potentials derived from pseudopotential theory.[14] Unfortunately, whilst these calculations are closer to first principles, they are not yet able to predict geometries and energies quantitatively. Thus for the self-interstitial in Al, with the use of such potentials, a minimal knock-on energy for induced diffusion of 0.15 eV is reported,[15] suggesting that the activation energy for self-diffusion (which should be a factor of 2 lower) is well below 0.1 eV, instead of the experimental value of 0.12 eV. Furthermore, for those situations which are interesting in the context of tunneling (i.e., where the classical activation energies and jump distances are sufficiently small), changes in the cutoff procedure can alter drastically the geometry for these potentials.

To obtain a reasonable estimate for the tunnel frequency in a given system, therefore, one has to correlate as many experimental data as possible to some potential parameters. This can best be done with a simple empirical potential, such as (2.1). Calculations have further shown that, if this is done, the main feature of the dynamics (such as resonant modes) do not depend strongly on the underlying model.[4]

## III. CALCULATION OF TUNNELING RATES

### A. Tunneling rates at 0 K: Methods

In the preceding section we discussed the static properties of interstitials and the way in which they are modeled. We now turn to their dynamic behavior. At the absolute zero of temperature, only a "tunneling" contribution remains, and the

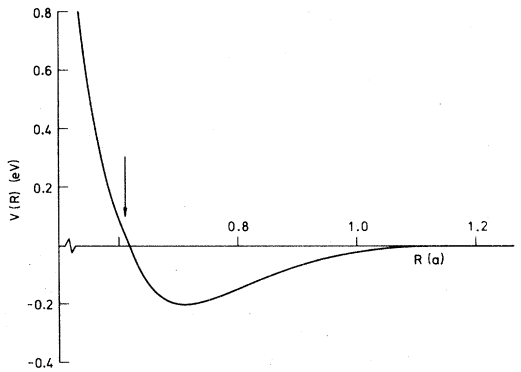


FIG. 2. Impurity-host potential for a tilted mixed-dumbell configuration. Arrow indicates the deviation from the smooth Morse potential. Parameters: $\delta = 0.005a$, $A = 0.02$ eV, $b = 0.02a$, $R_0 = 0.61a$. Potential shown corresponds to case 2(c) in Table II.

appropriate rate must be obtained from a solution of the Schrödinger equation. Provided the rate is small, one can write $\nu_T$, the tunnel frequency between two sites, in the form

$$h\nu_T = \frac{2[E_0\langle\psi_1|\psi_2\rangle - \langle\psi_1|H|\psi_2\rangle]}{1-\langle\psi_1|\psi_2\rangle^2}, \quad (3.1)$$

in which $E_0$ is $\langle\psi_1|H|\psi_1\rangle$ (or equivalently $\langle\psi_2|H|\psi_2\rangle$), and $H$ the Hamiltonian.

### 1. Initial and final states

It is vital to choose the right states between which the transitions occur. In this case $\psi_1$ and $\psi_2$ are ground-state wave functions of multidimensional harmonic oscillators. The oscillators describe the vibrations about the relaxed initial interstitial configuration ($\psi_1$) and final configuration ($\psi_2$). The Hamiltonian $H$ contains all the atomic kinetic energies and the full interaction described in the static calculations.

It is known that harmonic-oscillator ground-state wave functions result in an underestimate of the overlap in one-dimensional calculations. This will also be true to some extent in the multidimensional case. The error should, however, be less than in one dimension, since the overlap per mode will be larger and, therefore, will not depend as critically on the extreme wings of the wave functions. From Table IV, later in this paper, it can be seen that the values obtained in an effective one-dimensional approximation are only weakly affected by this choice of wave functions. The main point of the paper is to show the importance of the lattice coupling on the tunneling and, for this, the fine details of the wave functions are not important.

An important point to note is that specific atoms change their role between the initial and final states. For example, consider a jump from along the $+z$ direction to along the $+y$ direction of an impurity interstitial in an octahedral cage. In the initial state the host atom along $+z$ is part of a dumbbell: Afterwards, it is merely a host atom close to an impurity dumbbell. Because of this change in role of specific atoms, the normal modes also change in the transition. This change must be recognized in the calculations, even though there are symmetry operations (translations and rotations) which relate the initial and final states.

It is easily seen, for example, by using continuum elasticity, that the important atoms in $h\nu_T$ are the ones whose displacements change appreciably. For this reason, we can concentrate on the modes of a central cluster of atoms. Usually a 22-atom cluster is used, so that there is always a full set of host atoms around each dumbbell. Smaller clusters give too high a resonance frequency; indeed, the frequency may be used to monitor convergence with cluster size. In practive we choose the cluster by evaluating the overlaps between the initial and final state in the Einstein model for each atom separately, and by including all those atoms with overlaps significantly less than unity in the cluster. The contribution of the other atoms (i.e., those with overlaps very close to unity) is calculated for each one separately in the three-dimensional Einstein model.

### 2. Matrix elements of interatomic potentials

The evaluation of the matrix elements in (3.1) by direct, multidimensional, numerical integration would be very time consuming, and would introduce uncontrolled numerical errors. This difficulty is avoided by approximating $V(R)$ by Gaussians. Two methods of approximation were used. In the piecewise Gaussian fit we chose

$$V_p(R) = A_i \exp(-a_i R^2) - B_i \exp(-b_i R^2) + C_i . \quad (3.2)$$

The parameters $(A_i, B_i, C_i, a_i, b_i)$ give an essentially exact fit over a small range $R_i \le R \le R_i'$. The values of the parameters are therefore different for different pairs of atoms depending on their average distance $R_i \le R_{\text{av}} \le R_i'$. This approximation can become poor if there is a large change in distance between initial and final state. In these cases we used instead a whole-range Gaussian fit,

$$V_w(R) = A \exp(-aR^2) - B \exp(-bR^2) . \quad (3.3)$$

There the agreement is not so good locally, but is acceptable over a wide range of $R$. The replacement of $V$ by $V_w$ produces a 10% error in the calculated classical activation energy of the self-interstitial.

For convenience we replaced the small perturbing potential (2.2), which causes the tilting of the dumbbell, by a potential fixed in space and acting on the impurity only:

TABLE I. Tunnel splittings for different interstitial configurations. In these expressions $\Delta E$ is the tunnel splitting for two adjacent positions, ignoring all others, calculated with Eq. (3.1).

| Configuration | Symmetry | Energy |
|---|---|---|
| 1. Octahedral cage [Fig. 1(a)] | $E_g$ | $E_0+\Delta E$ |
| | $T_u$ | $E_0$ |
| | $A_g$ | $E_0-2\Delta E$ |
| 2. Cubic cage [Fig. 1(b)] | $A_u$ | $E_0+3\Delta E$ |
| | $T_g$ | $E_0+\Delta E$ |
| | $T_u$ | $E_0-\Delta E$ |
| | $A_g$ | $E_0-3\Delta E$ |
| 3. Split octahedral, with tilted dumbell [Fig. 1(c); there are two independent types of tunneling corresponding to $\nu_1$ (shorter) and to $\nu_2$ (longer), with $h\nu_1 \gg h\nu_2$]. | Longer range: As in (1) above, with $\Delta E \equiv h\nu_2$ | |
| | Shorter range: The interstitial stays in the same site but changes tilt direction, $\Delta E \equiv h\nu_1$ | |
| | $B_g$ | $E_0+2\Delta E$ |
| | $E_u$ | $E_0$ |
| | $A_g$ | $E_0-2\Delta E$ |

$$V_{\text{add}} = A\,[\exp(-a^2x^2)+\exp(-a^2y^2)]\ . \tag{3.4}$$

The initial- and final-state configurations were always recalculated using the Gaussian approximations, and all values given in the tables refer to this approximation.

Another ingredient concerns the normal modes, which can be obtained directly. For the contribution of the atoms at the outside of the cluster we have used the Einstein approximation, choosing the appropriate frequencies from the second derivatives of the potentials at the sites in question (and including here interaction with atoms outside the cluster).

Before we discuss the results for $h\nu_T$, we note three further points. Firstly, we have assumed tunneling is only important between adjacent sites. Thus we ignore transitions within an octahedral cage from along $+z$ to along $-z$, for example. Secondly, if the interstitial can move over $N$ sites, the $N$ degenerate levels in the absence of tunneling are split once tunneling is included. If we obtain a tunnel splitting $\Delta\epsilon$ for two sites considered by themselves, the splittings which result are those shown in Table I. Thirdly, it is convenient to express the results for $h\nu_T$ in a form which allows us to relate the full tunneling model to simple one-dimensional approximations. We shall write

$$\Delta E = 2\pi\hbar A \exp(-\sqrt{m_{\text{eff}}}B) \tag{3.5}$$

and discuss $A$ and $B$. Here $A$ is dimensionally a frequency, and $\exp(-\sqrt{m_{\text{eff}}}B)$ will be identified with the overlap $\langle\psi_1 \mid \psi_2\rangle$ of the initial and final states.

### B. Quantum tunneling at 0 K: Results

#### 1. *Dependence on host and impurity mass*

In order to interpret the results in terms of formula (3.5), we have varied the host and impurity masses. First, with both equal ($m_i = m_0$) we derive $\Delta E$ for a range of values of this mass. We then use Eq. (3.5) to derive $A$ and $B$ by fitting. To within 1% or 2%, this gives the value of $B$ derived from the overlap alone,

$$\langle\psi_1 \mid \psi_2\rangle = \exp(-\sqrt{m_0}B)\ ,\quad m_i = m_0\ . \tag{3.6}$$

Table II gives the values of $A$ and $B$ for a number of configurations. The configurations are characterized by their geometry, tunneling distance ($2d$) and classical activation energy ($E_a$).

If we only change the impurity mass, we can calculate an effective mass $m_{\text{eff}}$ from the overlap:

$$\langle\psi_1 \mid \psi_2\rangle = \exp(-\sqrt{m_{\text{eff}}}B)\ , \tag{3.7}$$

Table II. Tunneling constants and effective masses.

| Case | Configuration | $2d$ ($a$, i.e., 4.04 Å for Al) | $E_a$ (meV) | $A$ (THz) | $B$ (atomic mass units$^{-1/2}$) | $X$ |
|---|---|---|---|---|---|---|
| 1(a) | Octahedral | 0.288 | 108 | | 18.96 | 3.1 |
| 1(b) | | 0.240 | 39 | 306 | 12.24 | 2.9 |
| 1(c) | | 0.127 | 1.3 | 51 | 1.91 | 2.2 |
| 1(d) | | 0.093 | $<1$ | 29 | 1.025 | 2.5 |
| 2(a) | Split octahedral | 0.065 | 44 | 26 | 1.055 | 0.9 |
| 2(b) | | 0.092 | 10 | 32 | 1.28 | 1.4 |
| 2(c) | | 0.062 | 8 | 19 | 0.64 | 1.2 |
| 3 | Cubic | 0.127 | 3 | 58 | 2.37 | 2.70 |

$$m_{\text{eff}}=\frac{(m_i+Xm_0)}{(1+x)}\ , \tag{3.8}$$

where $X$ measures the extent to which the host atoms participate. The values of $X$ shown in Table II are calculated for $m_0=27$ and $m_i=60$. In all cases the value of $X$ increases with increasing impurity mass. For $m_i=40$, $X$ would be typically $5-10\,\%$ lower. This shift of $X$ can be understood qualitatively from the frequency shifts with changing mass. In almost all cases the effective mass corresponds to the participation of two to three host atoms in the reaction coordinate. This is the value expected for resonant libration modes.[16] The low value for the case of the split-octahedral cage is probably due to the approximation (3.4), where we replaced part of the impurity-host potential by a potential fixed in space.

### 2. *Magnitudes of prefactors*

The variation of the prefactor $A$ with impurity mass and host mass never exceeded 10%, and in most cases the change was below the numerical accuracy. We may conclude therefore that Eq. (3.5) is suitable to parametrize the tunnel splittings for a large range of geometries and masses. Detailed comparisons show that $2\pi\hbar A>\hbar\omega_R\gg\Delta E$ in all cases. The values of the resonance frequencies range from $1\times10^{13}$ to $2.5\times10^{13}$ cps. Even though the resonance modes dominate, the prefactor $A$ is not simply the frequency of the resonance mode, as one might have expected from some classical theories.

### 3. *Overlaps of initial and final states*

For our perturbation treatment to hold, one hopes the overlap $\langle\psi_1\,|\,\psi_2\rangle$ will be small. We may break this into several components:

(i) the overlap $S_R$ associated with the resonant mode(s),

(ii) the overlap $S_I$ associated with the cluster, including the resonant mode contribution, and

(iii) the overlap $S_B$ associated with the boundary atoms.

The total overlap is $\langle\psi_1\,|\,\psi_2\rangle=S_IS_B$ (or equivalently $B=B_I+B_B$). If one hopes to be able to make the simplest approximations to interstitial dynamics, one needs $S_B\sim1$, $S_I\sim S_R\ll1$. Table III

TABLE III. Breakdown of the overlap into its several contributions; $m_i=m_0=27$.

| Case | $\langle\psi_1\,\|\,\psi_2\rangle$ | $S_I$ | $S_B$ | $B_I$ | $B_R$ |
|---|---|---|---|---|---|
| 1(a) | $1.7\times10^{-43}$ | $6.5\times10^{-42}$ | 0.03 | 18.3 | 11.4 |
| 1(b) | $2.3\times10^{-28}$ | $6.3\times10^{-25}$ | $3.7\times10^{-4}$ | 10.7 | 8.9 |
| 1(c) | $4.7\times10^{-5}$ | $2.9\times10^{-4}$ | 0.15 | 1.6 | 1.4 |
| 1(d) | $4.9\times10^{-3}$ | $1.4\times10^{-2}$ | 0.33 | 0.82 | 0.72 |
| 2(a) | $4.1\times10^{-3}$ | $6.6\times10^{-3}$ | 0.63 | 0.97 | 0.62 |
| 2(b) | $1.3\times10^{-3}$ | $3.1\times10^{-3}$ | 0.41 | 1.11 | 1.05 |
| 2(c) | $3.5\times10^{-2}$ | $5.3\times10^{-2}$ | 0.66 | 0.56 | 0.44 |
| 3 | $4.4\times10^{-6}$ | $2.6\times10^{-5}$ | 0.17 | 2.0 | 1.8 |

shows $S_I$ to be small, as desired, with $S_B$ normally in the range $0.1-1$.

The contribution from the resonance modes gives an effective value of $B$ as

$$B_R=\sum_R \frac{1}{\hbar}\omega_R d_R^2, \quad m_i=m_0 \tag{3.9}$$

where $d_R$ is the mode half-jump distance. If the eigenvector of the mode $R$ is $\vec{e}_R$, and if the atomic displacements in the transition are $2\vec{d}$, then $d_R$ is defined by

$$d_R^2=|\vec{d}\vec{e}_R|^2 . \tag{3.10}$$

In Table III the effective values of $B_I$ are compared with the ones calculated from the resonant modes alone. The results confirm that the resonant modes dominate the behavior, though other motion cannot be ignored. These other contributions are especially important in those cases where the classical activation energies are high and the tunneling distances large.

## IV. SIMPLE APPROXIMATIONS FOR TUNNELING RATES OF $T=0$

The full atomistic calculations of the tunneling frequencies involve substantial amounts of work. It is therefore appropriate to see if one can obtain reasonable estimates merely from the much simpler calculations of the classical activation energy and frequency of the reaction coordinate. In this section therefore we look at some of the simple models which have been used to estimate tunneling rates at $T=0$. Such models are derived from simple one-dimensional potentials either by an exact solution, or by perturbation-theory equation (3.1) or by WKB theory.[17]

In all formulas the critical parameter (apart from numerical constants varying from case to case) is $\sigma$, the ratio of the classical activation energy to the vibration energy:

$$\sigma=m\omega d^2/\hbar \tag{4.1}$$

with $d$ the half-jump distance and $\omega$ defined by the potential-energy surface near the initial (or final) site. All the results given here assume $\sigma\gg 1$, and that $\sigma$ is obtained from atomistic calculations of classical activation and phonon energies.

Two different potential shapes are considered mainly in the literature: parabolic potential wells and a sinusoidal potential.

(i) parabolic potential wells:

$$V(x)=\mp\begin{cases}\frac{1}{2}m\omega^2(x-d)^2, & x>0\\ \frac{1}{2}m\omega^2(x+d)^2, & x<0 .\end{cases} \tag{4.2}$$

By expansions of the exact solution one obtains[18]

$$\Delta E=\hbar\omega\frac{2}{\sqrt{\pi}}\sqrt{\sigma}e^{-\sigma}=\hbar\omega 1.1284\sigma^{1/2}\exp(-\sigma) . \tag{4.3}$$

The same result is also obtained by perturbation-theory equation (3.1). Apart from a small numerical factor, the result is also reproduced with the use of the approximate WKB formula of Landau and Lifshitz[17]:

$$\Delta e=\left[\frac{e}{\pi}\right]^{1/2}\hbar\omega\frac{2}{\sqrt{\pi}}\sqrt{\sigma}e^{-\sigma}$$
$$=\hbar\omega 1.0496\sigma^{1/2}\exp(-\sigma) . \tag{4.4}$$

(ii) sinusoidal potential:

$$V(x)=\tfrac{1}{2}E_a\left[1+\cos\left[\frac{\pi}{d}x\right]\right]$$
$$=\frac{m\omega^2 d^2}{\pi^2}\left[1+\cos\left[\frac{\pi}{d}x\right]\right] . \tag{4.5}$$

The exact solution can be given in terms of Mathieu functions. In the limit $\sigma\ll 1$ an expansion of their characteristic values[19] gives[20]

$$\Delta E=\hbar\omega(2/\pi^{3/2})\sqrt{\sigma}\exp[-(8/\pi^2)\sigma]$$
$$\simeq\hbar\omega 0.3592\sigma^{1/2}\exp(-0.81060\sigma) . \tag{4.6}$$

In first-order perturbation theory one obtains the slightly different form

$$\Delta E=\hbar\omega\left[1-\frac{4}{\pi^2}\right]\sigma e^{-\sigma}$$
$$\simeq\hbar\omega 0.5947\sigma\exp(-\sigma) . \tag{4.7}$$

In WKB theory[17] one gets the result (4.6), apart from a factor $1/\sqrt{\pi}\simeq 0.5642$. The asymptotic solution to the Mathieu equation given in Morse and Feshbach[19] gives the result (4.6) instead of (4.5).

All models have the exponential dependence on $\sigma$ in common and therefore depend exponentially on $\sqrt{m}$. The prefactor has at most a weak dependence on $m$. One has to remember that terms like $\hbar\omega\sim m^{-1/2}$ have been omitted and must be handled separately. There is quite a variance in the numerical factors.

TABLE IV. Comparison of different approximations.

| Case | Multidimensional cluster Perturbation theory (3.1) | | Sine potential in one dimension Perturbation theory (4.7) | | Expansion (4.6) | |
|---|---|---|---|---|---|---|
| | $B$ | $\nu_T$ (THz) | $B$ | $\nu_T$ (THz) | $B$ | $\nu_T$ (THz) |
| 1(a) | 18.96 | | 13.65 | $1\times10^{-29}$ | 11.06 | $6\times10^{-29}$ |
| 1(b) | 12.24 | $7\times10^{-14}$ | 5.78 | $2\times10^{-12}$ | 4.69 | $8\times10^{-11}$ |
| 1(c) | 1.91 | $2\times10^{-3}$ | 0.59 | $4\times10^{-2}$ | 0.48 | $2.6\times10^{-2}$ |
| 1(d) | 1.025 | $1\times10^{-2}$ | $<0.38$ | $9\times10^{-2}$ | $<0.31$ | $5.9\times10^{-2}$ |
| 2(a) | 1.055 | $1\times10^{-1}$ | 1.32 | $3.3\times10^{-2}$ | 1.06 | $2.9\times10^{-2}$ |
| 2(b) | 1.28 | $4\times10^{-2}$ | 0.99 | $4.1\times10^{-2}$ | 0.80 | $2.9\times10^{-2}$ |
| 2(c) | 0.64 | $7\times10^{-1}$ | 0.57 | $2.9\times10^{-1}$ | 0.46 | $1.8\times10^{-1}$ |
| 3 | 2.37 | $3\times10^{-4}$ | 0.97 | $1.4\times10^{-2}$ | 0.78 | $1.6\times10^{-2}$ |

In Table IV we compare the values obtained for the exponential factor $B$ equation (3.5) and for the tunnel frequency $\nu_T$ ($m_i=m_0=27$) for the two one-dimensional approximations (4.5) and (4.6) to the multidimensional cluster result. As activation energy we use the values of Table III; the tunnel distance $d$ in the one-dimensional approximations we replace by an effective tunnel distance $d_{\text{eff}}$:

$$d_{\text{eff}}=d\sqrt{(1+X)}\ , \tag{4.8}$$

where $d$ and $X$ are given in Table II also. This corresponds to taking an effective mass.

One can see from Table IV that the one-dimensional values agree quite well with the cluster values. The complete failure for the cubic cage (case 3) occurs because the energy surface bears no resemblance to the assumed sine form. The same is true for the octahedral cage near its instability [case 1(d)]. We conclude that the one-dimensional formulas can be used to extrapolate the cluster values to different values of $E_a$, $d$, and $m$ as long as one is not too near to an instability.

## V. EXTENSION TO $T\neq0$ K

In this section we merely outline how to proceed from our present results to those at $T\neq0$. At elevated temperatures there will still be tunneling transitions between equivalent states $\psi_1$ and $\psi_2$. These can be calculated from Eq. (3.1) inserting excited states and thermal occupation numbers for them. With increasing temperature these coherent tunneling transitions will rapidly lose in importance compared with incoherent transitions, i.e., transitions where $\psi_1$ and $\psi_2$ are nonequivalent states of the whole crystal. In the limit of very high temperatures these latter transitions give rise to Arrhenius-type behavior of the diffusion constant. Much, though not all, of the formalism for these transitions can be taken over from Flynn and Stoneham.[22]

The diffusion rate can be expressed in terms of nonradiative transition probabilities of the form

$$w_{pp'}(ll')=\frac{2\pi}{\hbar}\,|\langle pl\,|\,H-E_{pl}\,|\,p'l'\rangle\,|^2\delta(E_{pl}-E_{p'l'})\ . \tag{5.1}$$

Here $H$ is the full Hamiltonian, $E_{pl}$ is the expectation value,

$$E_{pl}=\langle pl\,|\,H\,|\,pl\rangle\ , \tag{5.2}$$

and the $\delta(x)$ function ensures energy conservation. We have denoted by $p,p'$ the initial and final configuration and by $l,l'$ the occupation numbers of the eigenstates. The transition probability of interest is for neighboring interstitial sites $p,p'$, and is thermally averaged over the initial-state variables $l$ and summed over the final-state variables $l'$,

$$W'_{pp}=\sum_{l'}\langle w_{pp'}(l,l')\rangle_l\ . \tag{5.3}$$

The coherent terms $l=l'$ have to be omitted from the above formulas. The matrix elements in (5.1) can be calculated for a cluster of atoms with the methods used in the $T=0$ K case. The high occupation numbers associated with low-frequency resonance modes cause some difficulty, but this can be overcome by use of recursion relations and computer algorithms for analytical differentiation.

An important point concerns energy conservation. The $\delta$ function of (5.1) is appropriate when one treats the whole crystal in detail. But in practice one treats only a small cluster in detail the remainder being treated very approximately. Energy transfer to and from this remainder must be al-

lowed for. This problem can be solved similarly to Flynn and Stoneham.[22] We make the assumption that the rest of the lattice is coupled linearly to the cluster of atoms treated in detail. This assumption is much weaker than the usual one assuming a linear coupling of the whole lattice to the impurity site. Linear coupling implies that the modes of the rest of the lattice are not changed in the transition $p \rightarrow p'$, though they will be displaced. We thus obtain the following approximation for (5.1):

$$w'_{pp}(ll') = \frac{2\pi}{\hbar} | \langle pl | H - E_{pl} | p'l' \rangle |^2 \times \sum_r | \langle a_p(r) | a_p(r') \rangle_{r'} |^2 \times \delta(E_{pl} - E_{p'l'} + E_r - E_{r'}) . \quad (5.4)$$

$p,p',l,l'$ now denote the states of the cluster only whereas $r,r'$ denote the states of the rest of the lattice. The $\delta$ function is thus replaced by a shape function. Numerous approximations are available in the literature.[23]

## VI. CONCLUSION

We have presented a method to calculate the tunnel behavior of interstitials in metals at $T=0$ K in first-order perturbation theory. The full coupling of the tunneling particle to the lattice is taken into account. The tunneling process for heavy interstitials is dominated by a small number of resonant vibration modes, so that simpler methods can be used for extrapolation. In the case of simply shaped energy surfaces, reasonable estimates for the tunnel frequencies can be gained from the knowledge of the resonant modes or the classical activation energies and the tunneling geometries. The quantitative values given suggest that tunneling should be observable in suitable interstitial impurity systems. Using the experimental values for Al:Fe ($E_a \sim 15$ meV, $d \sim 0.06a$),[5,7] the estimated tunnel frequency would be $\nu_T = 10^4 - 10^8$ Hz, depending on the actual geometry and the details of the potential surface. The method presented can be generalized to deal with the effects at $T \neq 0$ K.

## ACKNOWLEDGMENTS

One of the authors (H.R.S.) gratefully acknowledges the hospitality of the Theoretical Physics Division of AERE Harwell where part of the work was done. Some of the initial calculations of $V$ were begun in collaboration with Miss Christine Neat, whom we thank for her contribution.

[1]W. Mansel, G. Vogl, and W. Koch, Phys. Rev. Lett. 31, 359 (1973).
[2]W. Mansel, H. Meyer, and G. Vogl, Radiat. Eff. 35, 69 (1978).
[3]G. Vogl, W. Mansel and P. H. Dederichs, Phys. Rev. Lett. 36, 1497 (1976).
[4]P. H. Dederichs, C. Lehmann, H. R. Schober, A. Scholz, and R. Zeller, J. Nucl. Mater. 69-70, 176 (1978).
[5]W. Petry, G. Vogl, and W. Mansel, Phys. Rev. Lett. 45, 1862 (1980).
[6]K. -H. Robrock, in *Phase Transitions and Solute Redistributions in Alloys during Irradiation,* edited by F. V. Nolfi, Jr. (Elsevier, New York, 1982).
[7]L. E. Rehn, K. -H. Robrock, and H. Jaques, J. Phys. F 8, 1835 (1978).
[8]K. L. Hultman, J. Holder, and A. V. Granato, J. Phys. (Paris) 42, 753 (1981).
[9]V. I. Startsev, V. P. Soldatov, V. D. Natsik and V. V. Abraimov, Phys. Status Solidi A 59, 377 (1980); P. Feltham, Phys. Status Solidi B 98, 301 (1980); see also N. F. Mott, Philos. Mag. 1, 568 (1956).
[10]K. W. Ingle, R. C. Perrin, and H. R. Schober, J. Phys. F 11, 1161 (1981).
[11]H. R. Schober, J. Phys. F 7, 1127 (1977).
[12]R. Zeller and H. R. Schober, in *Lattice Dynamics,* edited by M. Balkanski (Flammarion, Paris, 1977), p. 383.
[13]K. -H. Robrock and H. R. Schober, J. Phys. (Paris) 42, 735 (1981).
[14]N. Q. Lam, N. V. Doan, L. Dagens, and Y. Adda, J. Phys. F 11, 2231 (1981).
[15]N. W. Lam, N. V. Doan, and Y. Adda, J. Phys. F 10, 2359 (1980).
[16]P. H. Dederichs and R. Zeller, in *Dynamical Properties of Point Defects in Metals* Vol. 87 of *Springer Tracts in Modern Physics,* edited by G. Höhler (Springer, Berlin, 1980).
[17]L. D. Landau and E. M. Lifshitz, *Quantum Mechanics* (Pergamon, Oxford, 1959).
[18]E. Merzbacher, *Quantum Mechanics* (Wiley, New York, 1970).
[19]J. Meixner and F. W. Schäfke, *Mathieusche Funktionen and Sphäroidfunktionen* (Springer, Berlin, 1954); M. Abramovitz and I. A. Stegun, *Handbook of Mathematical Functions* (Dover, New York, 1965), p. 727FF.
[20]K. W. Kehr, in *Hydrogen in Metals I,* Vol. 28 of *Topics in Applied Physics,* edited by G. Alefeld and J. Völkl (Springer, Berlin, 1978), p. 197.

[21]P. M. Morse and H. Feshbach, *Methods of Theoretical Physics* (McGraw-Hill, New York, 1953), p. 1407 ff.
[22]C. P. Flynn and A. M. Stoneham, Phys. Rev. B 1, 3966 (1970).
[23]A. M. Stoneham, *Theory of Defects in Solids* (Clarendon, Oxford, 1975), especially Sec. 10.7